

1 The transcription factor Zt107320 affects the dimorphic switch, growth and virulence of the fungal  
2 wheat pathogen *Zymoseptoria tritici*

3

4 Michael Habig, Sharon Marie Bahena-Garrido<sup>#</sup>, Friederike Barkmann, Janine Haueisen and Eva  
5 Holtgrewe Stukenbrock\*

6

7 Environmental Genomics, Christian-Albrechts University of Kiel and Max Planck Institute for  
8 Evolutionary Biology, Plön, Germany,

9

10 # Current address:

11 #National Research Institute of Brewing, 3-7-1 Kagamiyama, Higashi-Hiroshima, 739-0046 Japan

12

13

14 \*corresponding author: [estukenbrock@bot.uni-kiel.de](mailto:estukenbrock@bot.uni-kiel.de)

15

16 Running head: Zt107320 regulates virulence in *Z. tritici*

17

18 Keywords: Fungal dimorphism, incompatible host, Septoria leaf blotch, gene expression, pycnidia  
19 formation

20

21 Word count: 6136

22

## 23 **Summary**

24 *Zymoseptoria tritici* is a filamentous fungus causing Septoria tritici blotch in wheat. The pathogen has  
25 a narrow host range and infections of grasses other than susceptible wheat are blocked early after  
26 stomatal penetration. During these abortive infections the fungus shows a markedly different  
27 expression pattern. However, the underlying mechanisms causing differential gene expression during  
28 host and non-host interaction are largely unknown, but likely include transcriptional regulators  
29 responsible for the onset of an infection program in compatible hosts. In the rice blast pathogen  
30 *Magnaporthe oryzae*, MoCOD1, a member of the fungal Zn(II)<sub>2</sub>Cys<sub>6</sub> transcription factor family, has  
31 been shown to directly affect pathogenicity. Here, we analyse the role of the putative transcription  
32 factor Zt107320, a homolog of MoCOD1, during infection of compatible and incompatible hosts by *Z.*  
33 *tritici*. We show for the first time that *Zt107320* is differentially expressed in host versus non-host  
34 infections and that lower expression corresponds to an incompatible infection of non-hosts. Applying  
35 reverse genetics approaches we further show that Zt107320 regulates the dimorphic switch as well  
36 as the growth rate of *Z. tritici* and affects fungal cell wall composition *in vitro*. Moreover,  $\Delta Zt107320$   
37 mutants showed reduced virulence during compatible infections of wheat. We conclude that  
38 Zt107320 directly influences pathogen fitness and propose that Zt107320 regulates growth processes  
39 and pathogenicity during infection. Our results suggest that this putative transcription factor is  
40 involved in discriminating compatible and non-compatible infections.

41

## 42 Introduction

43 The fungus *Zymoseptoria tritici* (synonym *Mycosphaerella graminicola*) infects wheat and causes the  
44 disease Septoria tritici blotch. The pathogen is found worldwide where wheat is grown and can cause  
45 severe reduction in yield (Fones and Gurr, 2015). Upon infection, the fungus enters the leaf through  
46 stomata and establishes a hyphal network in the mesophyll. It propagates without causing visual  
47 symptoms for 7-14 days before inducing necrosis and producing pycnidia – asexual fructifications,  
48 where pycnidiospores are produced that can spread via contact or rain-splash to neighbouring leaves  
49 (Brading *et al.* 2002; Kema, G. H. J. *et al.* 1996; Ponomarenko A. S.B. Goodwin, G.H.J. Kema, 2011). *Z.*  
50 *tritici* has a heterothallic mating system and meiosis leads to the production of wind-borne  
51 ascospores that are considered to be the main primary inoculum (Kema *et al.* 1996; Morais *et al.*  
52 2016; Ponomarenko A. S.B. Goodwin, G.H.J. Kema, 2011). Recently, we could show that  
53 chromosomal inheritance is characterised by frequent chromosome losses and rearrangements  
54 during mitosis and a drive of accessory chromosomes during meiosis (Habig *et al.* 2018; Möller *et al.*  
55 2018), which may contribute to the genomic variation observed for *Z. tritici* (Grandaubert *et al.* 2017;  
56 Hartmann *et al.* 2017). Under experimental conditions, the fungus has a narrow host range infecting  
57 wheat and shows abortive infections on closely related non-host grass species like *Triticum*  
58 *monococcum* (Jing *et al.* 2008) and *Brachypodium distachyon* (Kellner *et al.* 2014; O'Driscoll *et al.*  
59 2015). However, the underlying determinants of host specialisation and host specificity of *Z. tritici*  
60 are largely unknown.

61 A previous study comparing the expression profiles of *Z. tritici* between early infection (4 days post  
62 infection) of the compatible host *T. aestivum* and the non-host *B. distachyon* revealed a set of 289  
63 genes that were similarly expressed in the two hosts, but differentially expressed compared to  
64 growth in axenic culture (Kellner *et al.* 2014). These genes are likely crucial for *Z. tritici* during  
65 stomatal penetration that occurs in same way in both hosts. However, 40 genes showed differential  
66 expression between host and non-host infections (Kellner *et al.* 2014) and are possibly involved in  
67 the discrimination of compatible and non-compatible host-pathogen interactions. The signalling and

68 regulatory networks responsible for these differential expression patterns are however unknown.

69 One of the differentially expressed genes encodes the putative transcription factor Zt107320.

70 Expression of *Zt107320* was significantly increased during infection of *T. aestivum* compared to the

71 early infection of *B. distachyon* (Kellner *et al.* 2014) suggesting a host-dependent regulation of the

72 gene.

73 *Zt107320* encodes a putative transcription factor belonging to the Zn(II)<sub>2</sub>Cys<sub>6</sub> family. This gene family

74 of transcription factors is exclusive to fungi (MacPherson *et al.* 2006; Pan and Coleman, 1990) and

75 many members play an important role in the regulation of fungal physiology. For example, Zn(II)<sub>2</sub>Cys<sub>6</sub>

76 transcription factors in *Magnaporthe oryzae*, *Fusarium oxysporum*, *Leptosphaeria maculans*,

77 *Parastagonospora nodorum* and *Pyrenophora tritici-repentis* are involved in the regulation of fungal

78 growth and pathogenicity (Fox *et al.* 2008; Galhano *et al.* 2017; Imazaki *et al.* 2007; Lu *et al.* 2014;

79 Rybak *et al.* 2017). Interestingly, the homolog of *Zt107320* in the rice blast pathogen *M. oryzae*,

80 MoCOD1, was shown to affect conidiation and pathogenicity (Chung *et al.* 2013). *MoCOD1* was found

81 to be upregulated during conidiation and appressorium formation at 72h post infection.

82 Furthermore, the deletion mutant  $\Delta$ *MoCOD1* showed defects in conidial germination and

83 appressorium formation. *In planta*, the mutant  $\Delta$ *MoCOD1* was attenuated in extending growth from

84 the first-invaded cells and caused markedly reduced symptoms when compared to the wildtype

85 (Chung *et al.* 2013).

86 Transcription factors, in general, regulate expression by integrating various signalling pathways and

87 represent interesting targets for dissecting causes and mechanisms of pathogenicity and host

88 specificity. In *M. oryzae*, a systemic approach was applied to characterise all 104 members of the

89 Zn(II)<sub>2</sub>Cys<sub>6</sub> family of transcription factors. Of these, 61 were shown to be involved in fungal

90 development and pathogenicity (Lu *et al.* 2014). Similarly, in the head blight causing fungus *Fusarium*

91 *graminearum* 26% of 657 tested transcription factors had an effect on the tested phenotypes

92 mycelial growth, conidia production and toxin production (Son *et al.* 2011). In summary, a number of

93 transcription factors, which play important roles in host infection and pathogenesis, have been

94 identified for several important crop pathogens (Chen *et al.* 2017; Okmen *et al.* 2014; Xiong *et al.*  
95 2015; Zhang *et al.* 2018; Zhuang *et al.* 2016). In *Z. tritici* however, only few regulatory genes have  
96 been characterised. Recently, two transcription factors ZtWor1 (Mirzadi Gohari *et al.* 2014) and ZtVf1  
97 (Mohammadi *et al.* 2017) were shown to be important regulators of development and virulence of *Z.*  
98 *tritici* during compatible infections of wheat, highlighting how transcription factors can be used to  
99 identify and dissect aspects of pathogenicity. ZtWor1 has been functionally characterised and  
100 appears to be involved in the cAMP-dependent pathway, upregulated during the initiation of  
101 colonization and involved in regulating effector genes (Mirzadi Gohari *et al.* 2014). ZtVf1, a  
102 transcription factor belonging to the C<sub>2</sub>-H<sub>2</sub> subfamily is required for virulence and its deletion leads to  
103 lower pycnidia density within lesions. Decreased virulence appears to be due to a reduced  
104 penetration frequency and impaired pycnidia differentiation (Mohammadi *et al.* 2017)

105 Based on the close homology of *Zt107320* to *MoCOD1* and its significantly different expression  
106 profile during host and non-host infections, we hypothesized that *Zt107320* plays an important role  
107 during early wheat infection of *Z. tritici*. Our results confirm that *Zt107320* affects virulence of *Z.*  
108 *tritici* during compatible infections and regulates the dimorphic switch as well as growth rate and cell  
109 wall properties of this important fungal plant pathogen.

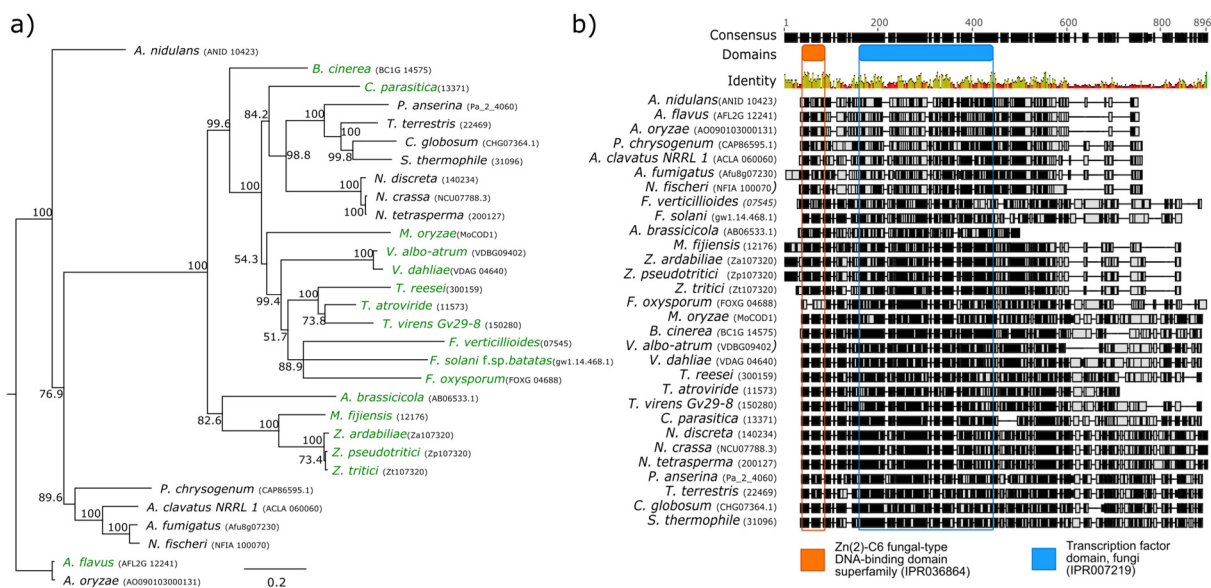
110

## 111 Results

### 112 Phylogenetic analysis of Zt107320

113 In order to determine the distribution of homologs of Zt107320 we performed a similarity search on  
 114 the protein level among putative fungal transcription factors. Among the 30 best matches 17 are  
 115 found among either plant pathogens or plant associated fungal organisms, however this association  
 116 does not appear to be monophyletic (fig 1 a). Among the thirty best hits, the *M. oryzae* homolog  
 117 MoCod1 and the *Alternaria brassicicola* homolog AbPf2 have been functionally analysed. Deletion of  
 118 the *AbPf2* resulted in non-pathogenic strains (Cho *et al.* 2013). In the wild-type expression of *AbPf2*  
 119 decreased after initial colonization of host tissues and the authors conclude that AbPf1 regulates  
 120 pathogenesis (Cho *et al.* 2013). Among these highly conserved putative transcription factors two  
 121 protein domains are shared: Zn(2)-C6 fungal-type DNA binding domain superfamily (IRP036864) and  
 122 the transcription factor domain (IRP007219), indicating a functional role of the putative transcription  
 123 factors (see fig. 1 b). Zt107320 is therefore homologous to several predicted transcription factors in  
 124 other fungal species, including some that have been associated with pathogenicity in plant  
 125 pathogenic species, indicating a similar regulatory role of this protein in *Z. tritici*.

126



127

128 **Figure 1. Homology of Zt107320 among fungal transcription factors.** a) Phylogenetic tree based on  
 129 30 sequences showing the highest similarity with Zt107320 on the protein level, including the  
 130 orthologs in the sister species *Z. pseudotritici* and *Z. ardabiliae*. The phylogenetic tree was

131 constructed using MUSCLE alignments (Edgar, 2004) with Neighbour-Joining upon a consensus tree  
132 with 1000 bootstrapping iterations. Support of nodes by percentage of bootstrapping iterations is  
133 indicated. Species considered to be associated with plants are indicated in green. B) MUSCLE  
134 alignment of homologous sequences to Zt107320 indicating regions according to their identity with  
135 the consensus sequence. The localisations of two functional domains, identified using InterProScan,  
136 in the consensus sequence are indicated.

137

138

139 **Infections of *Z. tritici* are blocked in the substomatal cavities during incompatible interaction with**  
140 ***B. distachyon* coinciding with reduced expression of *Zt107320***

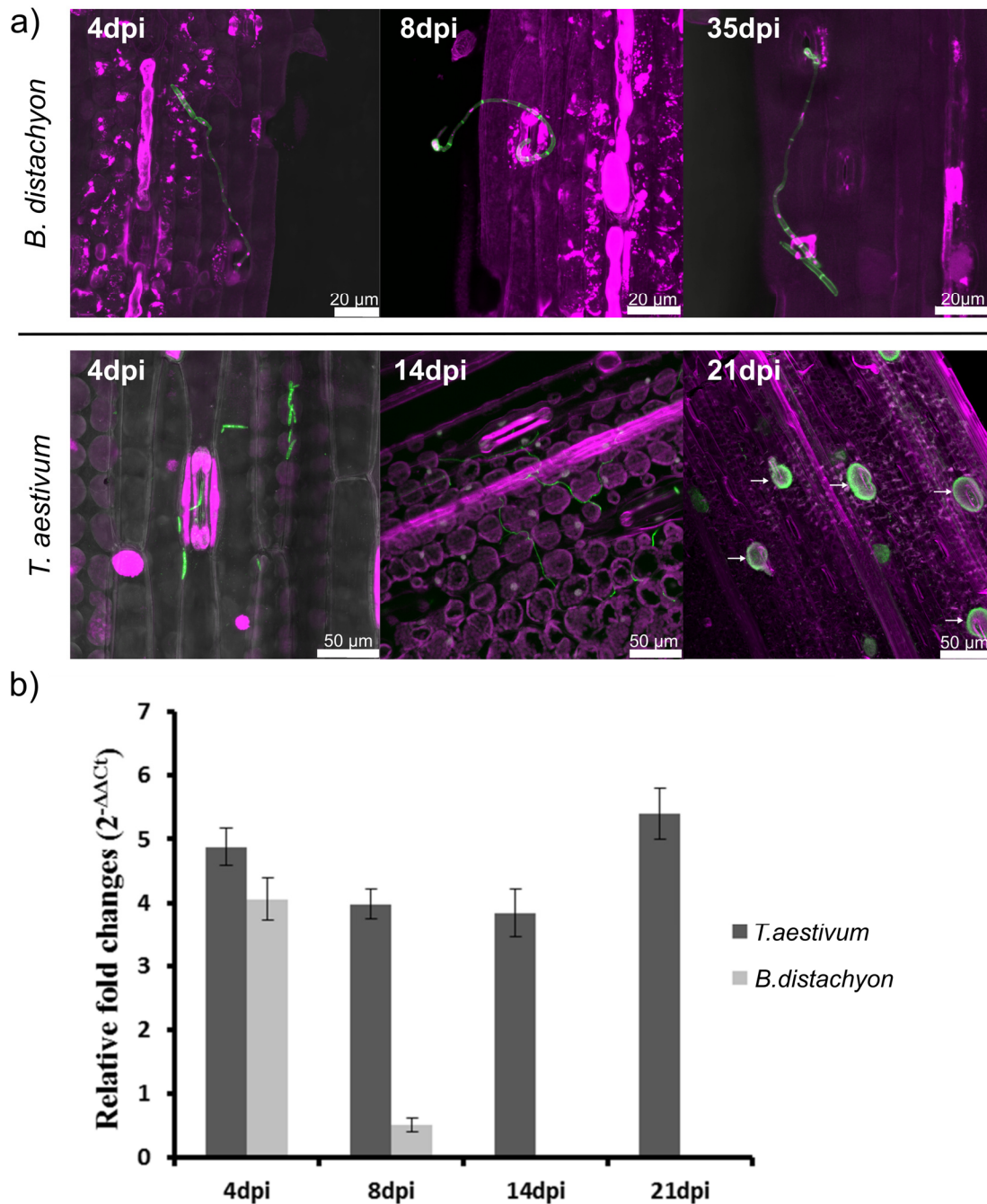
141 To study compatible and incompatible infections of *Z. tritici* in more detail, we inoculated leaves of  
142 12-14 days old seedlings of *T. aestivum* (cultivar Obelisk) and *B. distachyon* (ecotype Bd21), and  
143 analysed the infection development by confocal microscopy. Fungal cells germinated upon contact  
144 with the leaf surface and developed infection hyphae. In contrast to previous observations (O'Driscoll  
145 *et al.* 2015), we found that *Z. tritici* infection hyphae entered into open *B. distachyon* stomata at four  
146 days post inoculation (dpi). However, further infection development of *Z. tritici* was blocked in the  
147 substomatal cavities of *B. distachyon* leaves (fig 2a), similar to phenotypes previously observed in  
148 incompatible interactions with einkorn wheat (Jing *et al.* 2008). Consequently, *Z. tritici* hyphae did  
149 not colonize the mesophyll tissue of *B. distachyon*, no necrotic lesions developed, and no asexual  
150 pycnidia formed. Interestingly, fungal growth was completely halted and no further growth was  
151 observed, even when leaves were examined five weeks post inoculation (fig 2a). In contrast,  
152 compatible infection of *Z. tritici* on the wheat cultivar Obelisk was characterised by previously  
153 described infection stages (Haeisen *et al.* 2019). Penetration of leaf stomata at 4 dpi was followed  
154 by the establishment of a hyphal network in the mesophyll tissue until 7-11 dpi and subsequently the  
155 switch to necrotrophy when biomass increased substantially resulting in the formation of pycnidia  
156 (fig 2a).

157

158 Previously, comparative transcriptome analyses during *Z. tritici* infection of the host *T. aestivum* and  
159 the non-host *B. distachyon* identified 40 differentially expressed genes at 4 dpi (Kellner *et al.* 2014).  
160 Building on this expression analysis, we focused on the putative transcription factor Zt107320 and  
161 validated the expression kinetics of Zt107320 by RT-qPCR. We confirmed differential expression at 8  
162 dpi (fig 2b). Expression in the non-host *B. distachyon* was greatly reduced at 8 dpi compared to  
163 expression in axenic cultures, whereas the expression of Zt107320 during a compatible infection of  
164 the host *T. aestivum* was strongly upregulated during the course of the infection until 21 dpi.

165





166

167 **Figure 2. *Z. tritici* infection hyphae are blocked in the substomatal cavities of *B. distachyon* which**  
168 **coincides with reduced expression of *Zt107320*.** a) Micrographs showing *Z. tritici* cells and emerging  
169 hyphae during penetration of *B. distachyon* stomata and infection of *T. aestivum*. On *T. aestivum*, *Z.*  
170 *tritici* germinated and penetrated the stomata at 4 dpi. Intercellular mesophyll colonization of *Z.*  
171 *tritici* occurred until 14 dpi resulting in the formation of pycnidia (indicated by arrows) at 21 dpi. In  
172 contrast, *Z. tritici* germinated on *B. distachyon* and penetrated stomata, but growth was halted below  
173 the stomata with no further leaf colonization (8 dpi - 35 dpi). Maximum projections of confocal image  
174 z-stacks. Nuclei and grass cells displayed in purple and fungal hyphae or septae respectively in green.  
175 b) Transcription of *Zt107320* in compatible (*T. aestivum*) and incompatible (*B. distachyon*) hosts. *In*  
176 *planta* expression of *Zt107320* is displayed relative to expression during axenic growth. Values are

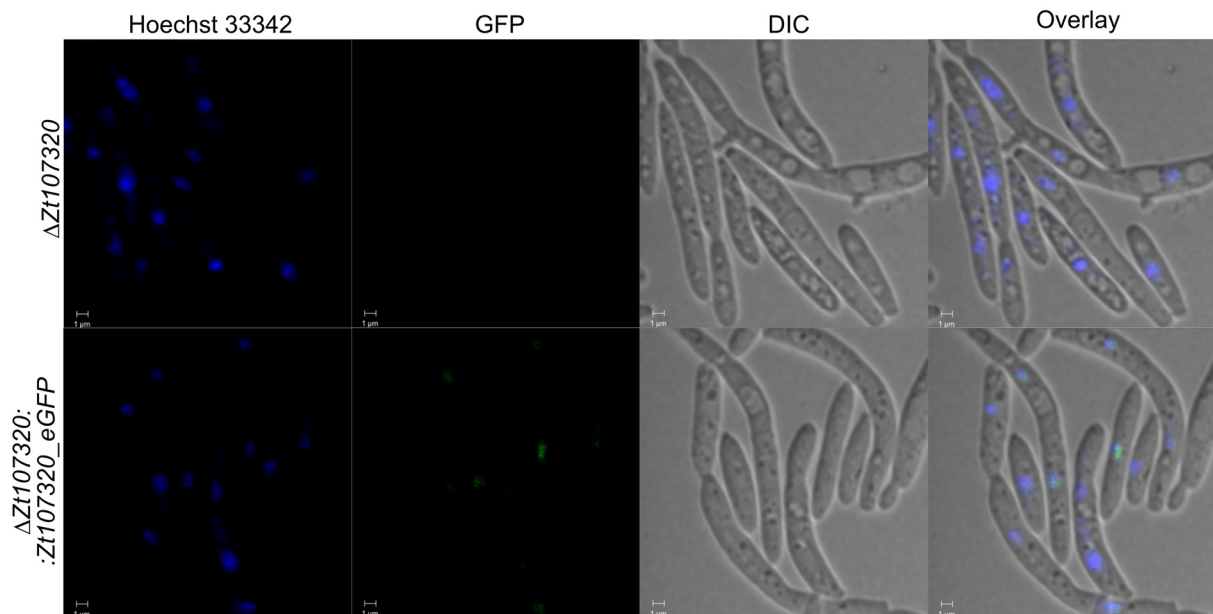
177 normalized to the expression of the gene encoding the housekeeping protein GAPDH. Error bars  
178 indicate the standard error of the mean (SEM) of three independent biological replicates per sample.

179

### 180 **Zt107320 is located with the nucleus during yeast-like growth**

181 The localization of Zt107320 within fungal cells was analysed using complementation strains that  
182 expressed a Zt107320\_eGFP fusion protein regulated by the native promotor. During yeast-like  
183 growth on YMS media, the GFP-fusion protein appeared to be located in the nucleus or in its  
184 immediate vicinity (see fig 3). This localization is similar to the reported nuclear localization of the  
185 homolog AbPf1 (Cho *et al.* 2013) and supports the putative functional role of Zt107320 as a  
186 transcription factor. The observed localisation of the Zt107320\_eGFP fusion protein also verifies the  
187 predicted nuclear localization of Zt107320 using the program WoLFPSort which implements an  
188 algorithm for prediction of subcellular locations of proteins based on sequence composition and  
189 content (Horton *et al.* 2007).

190



191

### 192 **Figure 3. Localization of the Zt107320\_eGFP fusion protein detected by fluorescence microscopy.**

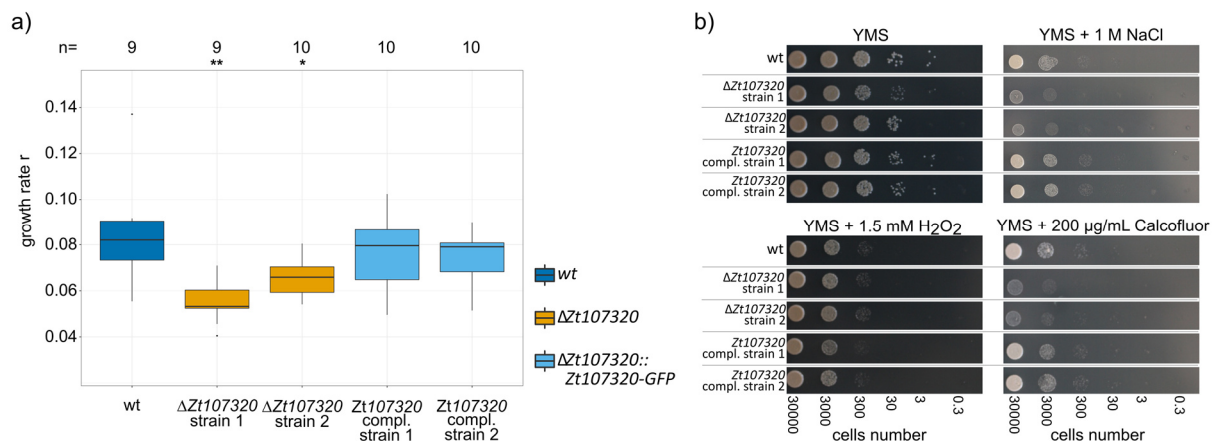
193 Nuclei were counterstained using the DNA-specific dye Hoechst33342. eGFP fluorescence co-  
194 localized with the Hoechst33342 signal indicating nuclear localization of the Zt107320\_eGFP fusion  
195 protein. eGFP fluorescence is restricted to the nuclei (scale bars = 1  $\mu$ m).

196

197 **Zt107320 regulates growth and affects cell wall properties**

198 Based on the coinciding halted growth and development and down-regulation of *Zt107320* in  
 199 incompatible infections, we next asked whether *Zt107320* is involved in the regulation of growth of  
 200 *Z. tritici* *in vitro*. We determined the maximum growth rate *r* of *Z. tritici* in liquid cultures assuming a  
 201 logistic growth curve model. For two independently generated *Zt107320* deletion mutants, we  
 202 observed a significant reduction in the maximum growth rate compared to the wildtype. We thereby  
 203 confirm the relevance of *Zt107320* as a putative regulator for growth, as two complementation  
 204 strains showed no significant difference in the growth rate compared to the wildtype (fig 4a)  
 205 The effect of *Zt107320* deletion was not restricted to the growth rate but also included cell wall  
 206 properties. Compared to the wildtype, we observed reduced growth *in vitro* when challenging the  
 207 deletion mutants with high osmotic stresses (0.5 M and 1 M NaCl; 1 M, 1.5 M and 2 M Sorbitol) as  
 208 well as with cell wall stress agents (300 µg/mL and 500 µg/mL Congo red; 200 µg/mL Calcofluor).  
 209 Again, the wildtype phenotype was restored in both complementation strains (fig 4b and fig S1).  
 210 Interestingly, temperature stress (28°C) did not affect the wildtype and the deletion mutants  
 211 differently, as well as the exposure to H<sub>2</sub>O<sub>2</sub> (1.5 mM and 2 mM). This indicates a specific effect of  
 212 *Zt107320* on the cell wall properties but not on the ability of the fungus to counteract reactive  
 213 oxygen species which are produced by the plant during activation of immune responses (Jones and  
 214 Dangl, 2006).

215



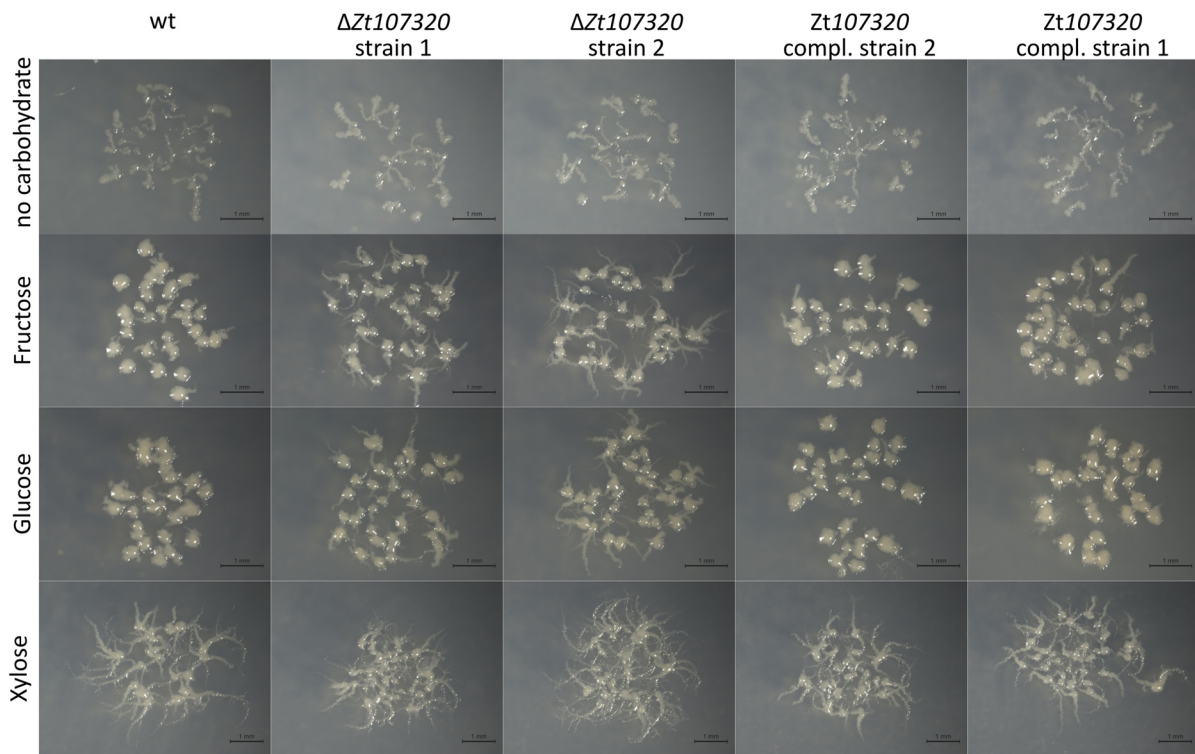
216

217 **Figure 4. Zt107320 regulates growth and affects cell wall properties of *Z. tritici*.** a) Maximum growth  
218 rate in liquid culture. Statistical significance inferred through an ANOVA and subsequent post hoc  
219 Tukey's HSD comparing the deletion and complementation strains to the wildtype, is indicated as \*=  
220  $p < 0.05$ ; \*\*=  $p < 0.005$ ; \*\*\*=  $p < 0.0005$ . b) *In vitro* growth of the wildtype (wt), two deletion strains  
221 ( $\Delta Zt107320$ ), two complementation strains ( $\Delta Zt107320::Zt107320\_eGFP$ ) on YMS media including  
222 the supplemented compounds to assess the role of osmotic stress (1 M NaCl), reactive oxygen  
223 species (1.5 mM H<sub>2</sub>O<sub>2</sub>) and cell wall stressors (200 µg/mL Calcofluor).

224

225 The dimorphic switch from yeast-like to hyphal growth is considered to be central for pathogenicity  
226 during the early stages of infection (Kema, G. H. J. *et al.* 1996; Yemelin *et al.* 2017). We therefore  
227 next asked whether Zt107320 is involved in regulating this morphological switch of *Z. tritici*. To  
228 promote hyphal growth we used minimal medium and supplied different carbon sources in order to  
229 compare carbon utilisation and growth between the mutants and wildtype. Without carbon sources  
230 as well as in the presence of cellulose as exclusive carbon source, *Z. tritici* showed solely hyphal  
231 growth, indicating that carbon sources are required for yeast-like growth and that cellulose cannot  
232 be utilized by the fungus. The wildtype *Z. tritici* strain showed markedly increased yeast-like growth  
233 in the presence of the monosaccharides glucose, galactose, fructose and mannose as well as the  
234 sugar alcohols sorbitol and mannitol. Increased growth was also observed in the presence of the  
235 disaccharides sucrose and maltose (fig 5, fig S2). Interestingly, xylose as sole carbon source led to  
236 predominant hyphal growth in the wild type strain, which contrasts to the mainly yeast-like growth  
237 observed in the presence of all other tested carbohydrates. For xylose as sole carbon source, overall  
238 growth is markedly increased compared to the minimal medium lacking a carbon source indicating  
239 that xylose can be utilized by *Z. tritici* as a carbon source. The deletion of *Zt107320* affected fungal  
240 growth morphology on all tested carbon sources. Compared to the wildtype and the  
241 complementation strains, we observed increased hyphal growth for the  $\Delta Zt107320$  strains on all  
242 carbon sources after 14 days of incubation, except for cellulose (fig 5, fig S2). In particular,  
243 supplementation of the monosaccharides fructose, glucose and xylose caused substantially  
244 pronounced hyphal growth when *Zt107320* was deleted. The wildtype phenotype was restored in

245 both complementation strains confirming that *Zt107320* plays a role in the regulation of growth in *Z.*  
246 *tritici*.



247

248 **Figure 5. *Zt107320* regulates the dimorphic switch of *Z. tritici*.** Pictures showing morphologies of  
249 colonies originating from single cells after 14 days of growth at 18°C on minimal media containing the  
250 indicated carbohydrates as carbon sources. Fructose, glucose and xylose can be utilized by the fungus  
251 and led to increased growth. The two strains in which *Zt107320* was deleted independently showed  
252 an increase in hyphal growth compared to the wildtype, while in the two complementation strains  
253 the wildtype colony morphology was restored.

254

### 255 ***Zt107320* affects the ability of *Z. tritici* to produce pycnidia**

256 We next addressed whether the impact of *Zt107320* deletion on growth rate, the dimorphic switch

257 and cell wall properties also influence the ability of *Z. tritici* to infect its host, *T. aestivum*. We

258 inoculated a predefined area of the second leaf of the susceptible wheat cultivar Obelisk and

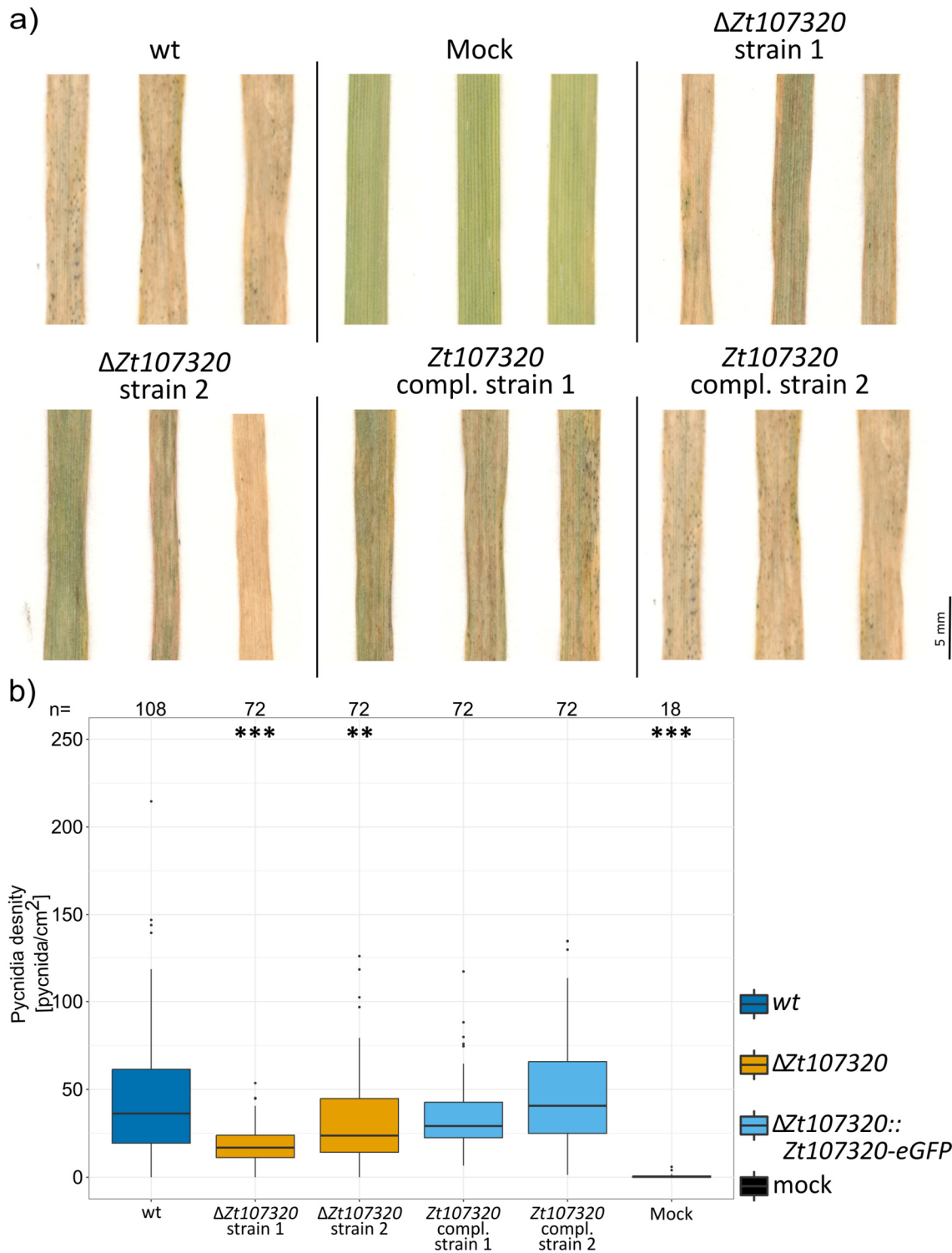
259 measured the number of pycnidia 21 days post infection. We observed a pronounced reduction in

260 the production of pycnidia for the *Zt107320* deletion strains. The density of pycnidia per cm<sup>2</sup> of

261 infected leaf area was reduced significantly for both independent deletions of *Zt107320* (ANOVA,

262  $p < 1 \cdot 10^{-7}$ ,  $p = 0.002$ ) (fig 6 a, b) compared to the wildtype. Complementing the *Zt107320* in-locus fully

263 restored the wildtype phenotype *in planta*. As the density of pycnidia is considered to be a  
 264 quantitative measure for virulence (Stewart *et al.* 2016), significantly decreased pycnidia production  
 265 indicates reduced virulence of mutants. Thus, we conclude that the putative transcription factor  
 266 Zt107320 by its effect on the growth rate, the dimorphic switch and the cell wall properties affects  
 267 the fitness of *Z. tritici* during infection of the compatible wheat host.



269 **Figure 6. *Zt107320* deletion affects the pycnidia production during a compatible infection of wheat.**  
270 a) Pictures of representative leaves infected with the *Z. tritici* wildtype (wt), two deletion strains  
271 ( $\Delta Zt107320$ ), two complementation strains ( $\Delta Zt107320::Zt107320-eGFP$ ) and mock-treated leaves. b)  
272 Boxplot depicting the pycnidia density (pycnidia per cm<sup>2</sup> leaf) pooled for two independent  
273 experiments. Number of leaves (N) for each strain is indicated on top. Statistical significance, inferred  
274 through an ANOVA and subsequent post hoc Tukey's HSD comparing the deletion and  
275 complementation strains to the wildtype, is indicated as \*= p <0.05; \*\*= p<0.005; \*\*\*= p<0.0005.

276

277

## 278 **Discussion**

279 Here, we show that the putative transcription factor *Zt107320*, belonging to the fungal Zn(II)<sub>2</sub>Cys<sub>6</sub>  
280 family, is involved in the infection program of *Z. tritici* during a compatible interaction with the host  
281 plant *T. aestivum*. Transcription of *Zt107320* is specifically induced during infection of wheat but not  
282 during the infection of the non-host *B. distachyon*. This suggests a functional role of this gene in the  
283 regulation of the infection program during a compatible host-pathogen interaction that allows the  
284 fungus to overcome host defences and propagate in the mesophyll tissue.

285 To date, only a small number of genes have been shown to be involved in virulence of this important  
286 wheat pathogen (Orton *et al.* 2011; Poppe *et al.* 2015). These genes encode the chitin binding LysM  
287 effector Mg3LysM (Lee *et al.* 2014; Marshall *et al.* 2011), two transcription factors *ZtWor1* and *ZtVf1*  
288 (Mirzadi Gohari *et al.* 2014; Mohammadi *et al.* 2017) and three rapidly evolving small proteins  
289 (Hartmann *et al.* 2017; Poppe *et al.* 2015; Zhong *et al.* 2017). Indeed, multiple effector candidate  
290 genes have been deleted but for most mutants no or small effects on pathogenicity were observed  
291 (Gohari *et al.* 2015; Rudd *et al.* 2015). Therefore, a high level of functional redundancy seems to be  
292 present in *Z. tritici*. The deletion of *Zt107320* results in a relatively small, nevertheless significant,  
293 reduction of the pycnidia density which is in contrast to the fully or partially avirulent phenotype  
294 demonstrated for the two previously deleted transcription factors *ZtWor1* and *ZtVf1*, respectively  
295 (Mirzadi Gohari *et al.* 2014; Mohammadi *et al.* 2017). Similar to our observation in the *Zt107320*  
296 deletion mutant, deletion of *MoCOD1*, the rice blast homolog of *Zt107320*, led to a quantitative  
297 reduction in lesion size and number (Chung *et al.* 2013). This partial, but incomplete, quantitative

298 reduction in virulence of  $\Delta Zt107320$  strains corresponds with the reduced, but still substantial  
299 growth rate of these deletion mutants *in vitro*. Therefore, other mechanisms, independent of  
300 Zt107320 are involved in the regulation of growth and development *in vitro* and *in planta*. Similarly, a  
301 partial, but incomplete reduction of invasive growth *in planta* as observed in  $\Delta MoCOD1$  (Chung *et al.*  
302 2013). The impact of Zt107320 on fungal growth and pathogenicity is therefore similar to the effect  
303 caused by other members of the Zn(II)<sub>2</sub>Cys<sub>6</sub> transcription factor family: TPC1 regulates invasive,  
304 polarized growth and virulence in the rice blast fungus *M. oryzae* (Galhano *et al.* 2017), and the  
305 transcription factor FOW2 is known to control the ability of *F. oxysporum* to invade roots and  
306 colonize plant tissue (Imazaki *et al.* 2007).

307 Zt107320 appears to be involved in the morphological switch from yeast-like to hyphal growth as  
308 deletion of *Zt107320* led to an increase in hyphal growth. The switch to filamentous growth is  
309 considered to be essential for plant infection (Kema, G. H. J. *et al.* 1996; Yemelin *et al.* 2017).  
310 Therefore, the involvement of Zt107320 in regulating this dimorphism underscores its importance for  
311 pathogenicity. Based on RT-qPCR data we observe that *Zt107320* is differentially expressed between  
312 non-host and host infections and is further highly expressed during infections of compatible hosts.  
313 Other RNAseq-based transcriptome studies found that *Zt107320* is upregulated during later stages of  
314 wheat infection associated to necrotrophic host colonization, indicating a possible function for  
315 pycnidia formation (Haueisen *et al.* 2019; Rudd *et al.* 2015). Together, these findings support a role  
316 of Zt107320 in regulation of growth and pathogenicity of *Z. tritici*.

317 Interestingly, xylose the main product of hemicellulose degradation by fungal xylanases had a  
318 pronounced effect on the growth pattern of *Z. tritici*. Xylose supplementation not only increased  
319 overall growth compared to pure minimal medium but also led to an increase in the development of  
320 filaments spanning larger distances. In *Z. tritici*, the switch to necrotrophic growth after an initial  
321 phase of symptomless infection, overall disease severity and quantitative pycnidiospore production  
322 are associated with the activity of endo- $\beta$ -1,4-xylanase (Siah *et al.* 2010; Somai-Jemmali *et al.* 2017).  
323 During the switch to necrotrophy *Z. tritici* rapidly develops large hyphal networks and uses plant-



324 derived nutrients (Haueisen *et al.* 2019; Rudd *et al.* 2015). The observed effect of xylose on the  
325 growth morphology suggest that xylose – next to its role as a carbon source – may also direct growth  
326 and promote the spatial expansion of the intrafoliar hyphal network during the fungal lifestyle switch  
327 to necrotrophic growth. Indeed, genes encoding xylanases were shown to evolve under positive  
328 selection (Brunner *et al.* 2013), indicating an important functional role of this class of enzymes for  
329 adaptation to wheat infection. Although functional analyses of several xylanases in other plant  
330 pathogenic fungi, resulted in no direct phenotypic effect (Brunner *et al.* 2013; Douaiher *et al.* 2007)  
331 xylanases have been proposed as virulence factors (Douaiher *et al.* 2007). However, the results  
332 presented here indicate a possible role of xylose as a host infection-associated signal molecule for *Z.*  
333 *tritici* and should warrant further analysis.

334 In conclusion, we showed that Zt107320 affects the fitness of the wheat pathogen *Z. tritici*. *Zt107320*  
335 is differentially expressed in host and non-host environments, being upregulated during the early  
336 stages of infection on compatible hosts and down-regulated on non-hosts. This down-regulation  
337 corresponds to a considerably reduced growth and halted infections of *Z. tritici* after stomatal  
338 penetration of the non-host *B. distachyon*. In addition, we could confirm that Zt107320 has a nuclear  
339 localisation, consistent with its putative function as a transcription factor and that it further regulates  
340 the dimorphic switch between yeast-like and hyphal growth that is considered to be essential for  
341 pathogenicity. We therefore hypothesize that the putative transcription factor Zt107320 is part of to  
342 the regulatory network that controls host-associated growth and development, integrating signals  
343 that differ between compatible and non-compatible infections. Future studies should address the  
344 specific target genes of Zt107320 and their expression pattern during compatible and non-  
345 compatible interactions. Furthermore, the transcriptional regulation of *Zt107320* suggests that  
346 specific signals in the compatible host-pathogen interaction in wheat are responsible for the up-  
347 regulation of this particular transcription factor-encoding gene. Identification of these host-derived  
348 signals will provide fundamental insight into the molecular basis of host-pathogen interaction and  
349 host specificity in *Z. tritici*.

350

## 351 **Experimental Procedures**

### 352 **Fungal and plant strains**

353 The Dutch isolate IPO323 was kindly provided by Gert Kema (Wageningen, The Netherlands) and is  
354 available from the Westervijk Institute (Utrecht, The Netherlands) with the accession number CBS  
355 115943. The strain used in our experiments lacked accessory chromosome 18, presumably lost  
356 during culture maintenance *in vitro* (Kellner et al. 2014). Strains were maintained in either liquid  
357 Yeast Malt Sucrose (YMS) broth (4 g/L Yeast extract, 4 g/L Malt extract, 4 g/L sucrose) at 18°C on an  
358 orbital shaker or on solid YMS (+20 g/L agar) at 18°C. The *T. aestivum* cultivar Obelisk was obtained  
359 from Wiersum Plantbreeding BV (Winschoten, The Netherlands). *B. distachyon* inbred line Bd21 was  
360 kindly provided by Thierry Marcel (Bioger, INRA, France).

361

### 362 **Sequence analysis**

363 Phylogenetic analysis of Zt107320 was conducted using the software Geneious Prime 2019.0.4  
364 (<https://www.geneious.com>). Homologues sequences to protein sequence of Zt107320 were  
365 retrieved from the Fungal Transcription Factor Database (Park *et al.* 2008). Including Zt107320 and its  
366 homologs from the sister species *Z. pseudotritici* and *Z. ardabiliae* a total of the 30 best matches  
367 were retrieved. Alignments were constricted using MUSCLE (Edgar, 2004) and trees constructed  
368 using Neighbour-Joining algorithm building a consensus tree using 1000 bootstrapping replicates.  
369 Protein domains of the consensus sequence were identified using InterProScan (Quevillon *et al.*  
370 2005). Prediction of the nuclear localisation of the Zt107320 was conducted using the WoLF PSORT  
371 predictor (Horton *et al.* 2007).

372

### 373 **Analysis of *Z. tritici* during its compatible and non-compatible infections by confocal microscopy**

374 Morphology and development of *Z. tritici* inside and on the surface of leaves of *B. distachyon* inbred  
375 line Bd21 were analysed by confocal laser-scanning microscopy (CLSM) as described previously  
376 (Haeuelsen et al. 2019). Analyses of compatible *Z. tritici* infections on *Triticum aestivum* cultivar  
377 Obelisk were conducted by combining microtomy and CLSM as previously described (Rath et al.  
378 2014). Distinct areas of the second leaf of 12-day-old (Bd21) and 14-day-old (wheat) seedlings were  
379 brush-inoculated with  $1 \times 10^7$  cells/ml in 0.1% Tween 20. Plants were incubated at 22°C [day]/ 20°C  
380 [night] and 100% humidity with a 16-h light period for 48 h. Subsequently, humidity was reduced to  
381 70%. Microscopy was conducted using a Leica TCS SP5 and analysis of image z-stacks was done using  
382 Leica Application Suite Advanced Fluorescence (Leica Microsystems, Germany) and AMIRA® (FEITM  
383 Visualization Science Group, Germany).

384

#### 385 **Analysis of Zt107320\_eGFP expression using confocal microscopy.**

386 Cells were grown on solid YMS medium for 7 days before being scraped off the media surface and  
387 introduced into 10 mM phosphate buffer (pH 7.2) containing 1 µg/µl Hoechst 33342 (Sigma-Aldrich  
388 Chemie GmbH, Munich, Germany). Cells were incubated for 15-30 min in the dark and then  
389 transferred to a microscope slide and analysed by confocal laser scanning microscopy.

390

#### 391 **RNA isolation and quantitative RT-PCR**

392 We analysed gene expression patterns of *Zt107320* of *Z. tritici* employing a qRT-PCR experiment.  
393 Total RNA was extracted from fungal axenic cultures (grown for 72 h in YMS medium at 18°C and 200  
394 rpm) and from snap-frozen leaf tissue infected with *Z. tritici* (4, 8, 14 and 21 dpi) using the TRIZOL  
395 reagent (Invitrogen, Karlsruhe, Germany), following the manufacturer's instructions. Three biological  
396 replicates were included in the experimental set up. The cDNA samples were used in a qRT-PCR  
397 experiment employing the iQ SYBR Green Supermix Kit (Bio-Rad, Munich, Germany). PCR was  
398 conducted in a CFX96 RT-PCR Detection System (Bio-Rad, Munich, Germany) with the constitutively

399 expressed control gene Glyceraldehyde-3-phosphate dehydrogenase (GAPDH). All primers are listed  
400 in table S1.

#### 401 **Generation of Zt107320 deletion mutants and complementation by gene replacement**

402 Fungal transformations and the creation of knock-out and complementation mutants of *Zt107320*  
403 were conducted as previously described (Poppe *et al.* 2015). In brief: Gene deletions were created by  
404 amplifying an approximately 1 kb region of the 5' and 3' flanking regions of *Zt107320* using PCR. The  
405 amplified flanking sequences were fused to a hygromycin resistance (hygR) cassette and an EcoRV  
406 cut vector backbone (pES61) using Gibson assembly (Gibson *et al.* 2009). Electro-competent cells of  
407 the *Agrobacterium tumefaciens* strains AGL1 were transformed using standard protocols. These  
408 transformed *A. tumefaciens* cells were used for the transformation of *Z. tritici* as previously described  
409 (Zwiers and De Waard, Maarten A. 2001). The same strategy was applied for the creation of the  
410 complementation strains by a C-terminal fusion of the *Zt107320* gene with an eGFP tag and a  
411 geneticin resistance cassette as a selection marker (fig. S3). After transformation and homologous  
412 recombination in the  $\Delta Zt107320$  strain 1, the hygromycin resistance cassette was replaced by  
413 *Zt107320-eGFP* and the geneticin resistance cassette (NeoR) (fig. S3). Homologous recombination  
414 and integration was confirmed using PCR and Southern blot analysis by standard protocols. In short,  
415 genomic DNA was isolated using Phenol-Chloroform isolation (Sambrook and Russell, 2001).  
416 Restriction digestion was performed using PvuII, followed by gel-electrophoresis, blotting and  
417 detection using Dig-labelled probes binding to the upstream and downstream flank of *Zt107320* (fig.  
418 S2). In total four  $\Delta Zt107320$  strains, and two  $\Delta Zt107320::Zt107320$ -eGFP strains were created.

419

#### 420 **Isolation of fungal DNA and Southern blot analysis**

421 DNA was isolated using phenol/chloroform applying a protocol previously described (Sambrook and  
422 Russell, 2001). Transformants were first screened using a PCR based approach detecting the  
423 resistance cassette and the endogenous locus. Candidate transformants were further confirmed by  
424 Southern blot analysis using a standard protocol (Southern, 1975). Probes were generated using the

425 PCR DIG labelling Mix (Roche, Mannheim, Germany) according to the manufacturer's instructions  
426 (Table S1).

427

#### 428 ***In vitro* phenotyping**

429 The *Z. tritici* strains were grown on YMS solid medium for 5-7 days at 18°C before the cells were  
430 scraped from the plate surface. For the determination of the growth rate, the cells were resuspended  
431 and counted. The cell density was adjusted to 50000 cells/mL and 175µl of the cell suspension was  
432 added to a well of a 96 well plate. Plates were inoculated at 18°C at 200 rpm with the OD600 being  
433 measured twice daily on a Multiskan Go plate reader (Thermo Scientific, Dreieich, Germany) (Table  
434 S2). Estimation of the growth rate was done by employing the logistic growth equation as  
435 implemented in the growthcurver package (version 0.2.1) in R (version R3.4.1) (R Core Team, 2015).  
436 For the determination of the *in vitro* phenotypes, the cell number was adjusted to 10<sup>7</sup> cells/mL in  
437 ddH<sub>2</sub>O and serially diluted to 10<sup>3</sup> cells/mL. 3 µL of each cell dilution was transferred onto YMS agar  
438 including the tested compounds and incubated for seven days at 18°C or 28°C. To test high osmotic  
439 stresses 0.5 M NaCl, 1 M NaCl, 1M Sorbitol, 1.5 M Sorbitol, 2 M Sorbitol (obtained from Carl Roth  
440 GmbH, Karlsruhe, Germany) were added to the YMS solid medium. To test cell wall stresses 300  
441 µg/mL and 500 µg/mL Congo red and 200 µg/mL Calcofluor (obtained from Sigma-Aldrich Chemie  
442 GmbH, Munich, Germany) were added to the YMS solid medium. Finally, to determine the effect of  
443 reactive oxygen species on the mutant growth morphology 2 mM H<sub>2</sub>O<sub>2</sub> (obtained from Carl Roth  
444 GmbH, Karlsruhe, Germany) was added to the YMS solid medium.

445 To test whether the Zt107320 affects the hyphal growth of *Z. tritici* and the ability of the fungus to  
446 use different carbon sources we used minimum media (MM) as described in (Barratt *et al.* 1965).  
447 Glucose, fructose, xylose, mannose, galactose, sorbitol, mannitol, sucrose and cellulose were added  
448 at a final concentration of 10 g/L and 20g/L agar were included. Strains were grown on YMS solid  
449 medium for 7 days and scraped into ddH<sub>2</sub>O, the cell number adjusted to 10<sup>7</sup>, 10<sup>6</sup>, 10<sup>5</sup>, 10<sup>4</sup>, 10<sup>3</sup>

450 cells/mL and 3  $\mu$ l of each cell concentration added to the surface of the minimum medium plates.

451 Plates were incubated 18°C in the dark and the growth monitored after 7 days and 14 days.

452

### 453 ***In planta* phenotyping**

454 For the *in planta* phenotypic assays, we germinated seeds of the wheat cultivar Obelisk on wet sterile

455 whatman paper for four days before potting using the soil Fruhstorfer Topferde (Hermann Meyer

456 GmbH, Rellingen, Germany). Wheat seedlings were further grown for seven days before inoculation.

457 *Z. tritici* strains were grown in YMS solid medium for five days at 18°C before the cells were scraped

458 from the plate surface. The cell number was adjusted to 10<sup>8</sup> cells/mL in H<sub>2</sub>O + 0.1% Tween 20, and

459 the cell suspension was brushed onto approximately five cm on the abaxial and adaxial sides of the

460 second leaf of each seedling. Inoculated plants were placed in sealed bags containing water for 48 h

461 to facilitate infection through stomata. Plants were grown under constant conditions with a day night

462 cycle of 16h light ( $\sim$ 200 $\mu$ mol/m<sup>2</sup>\*s) and 8h darkness in growth chambers at 20°C. Plants were grown

463 for 21 days post inoculation at 90% relative humidity (RH). At 21 dpi the infected leaves were cut and

464 taped to sheets of paper and pressed for five days at 4°C before being scanned at a resolution of

465 2400 dpi using a flatbed scanner (HP photosmart C4580, HP, Böblingen, Germany). Scanned images

466 were analysed using an automated image analysis in Image J (Schneider *et al.* 2012) adapted from

467 (Stewart *et al.* 2016). The read-out pycnidia/cm<sup>2</sup> leaf surface was used for all subsequent analyses.

468 See Table S3 for summary of *in planta* results.

469

### 470 **Statistical analysis**

471 Statistical analyses were conducted in R (version R3.4.1) (R Core Team, 2015) using the suite R Studio

472 (version 1.0.143) (RStudio Team, 2015). Data inspection showed a non-normal distribution for all

473 data sets, including the measured pycnidia density (pycnidia/cm<sup>2</sup>). Therefore, we performed an

474 omnibus analysis of variance using rank-transformation of the data (Conover and Iman, 1981)

475 employing the model: pycnidia density  $\sim$  strain \* experiment and  $r \sim$  strain, respectively. Post hoc  
476 tests were performed using Tukey's HSD (Tukey, 1949).

477

## 478 **Acknowledgements**

479 The study was funded by a personal grant to EHS from the State of Schleswig Holstein and a  
480 fellowship from the Max Planck Society, Germany. The funders had no role in study design, data  
481 collection and interpretation, or the decision to submit the work for publication. The authors have no  
482 conflict of interest.

483

## 484 **References**

- 485 **Barratt, R.W. Johnson, G.B. and Ogata, W.N.** (1965) Wild-type and mutant stocks of *Aspergillus*  
486 *nidulans*. *Genetics*, **52**, 233.
- 487 **Brading, P.A. Verstappen, Els C P, Kema, Gert H J and Brown, James K M** (2002) A Gene-for-Gene  
488 Relationship Between Wheat and *Mycosphaerella graminicola*, the Septoria Triticum Blotch  
489 Pathogen. *Phytopathology*, **92**, 439–445.
- 490 **Brunner, P.C. Torriani, S. F. F. Croll, D. Stukenbrock, E.H. and McDonald, B.A.** (2013) Coevolution  
491 and Life Cycle Specialization of Plant Cell Wall Degrading Enzymes in a Hemibiotrophic Pathogen.  
492 *Molecular Biology and Evolution*, **30**, 1337–1347.
- 493 **Chen, Y. Le, X. Sun, Y. Li, M. Zhang, H. Tan, X. Zhang, D. Liu, Y. and Zhang, Z.** (2017) MoYcp4 is  
494 required for growth, conidiogenesis and pathogenicity in *Magnaporthe oryzae*. *Mol. Plant Pathol.*  
495 **18**, 1001–1011.
- 496 **Cho, Y. Ohm, R.A. Grigoriev, I.V. and Srivastava, A.** (2013) Fungal-specific transcription factor AbPf2  
497 activates pathogenicity in *Alternaria brassicicola*. *The Plant journal : for cell and molecular biology*,  
498 **75**, 498–514.
- 499 **Chung, H. Choi, J. Park, S.-Y. Jeon, J. and Lee, Y.-H.** (2013) Two conidiation-related Zn(II)2Cys6  
500 transcription factor genes in the rice blast fungus. *Fungal Genet. Biol.* **61**, 133–141.
- 501 **Conover, W.J. and Iman, R.L.** (1981) Rank transformations as a bridge between parametric and  
502 nonparametric statistics. *The American Statistician*, **35**, 124–129.
- 503 **Douaiher, M.-N. Nowak, E. Durand, R. Halama, P. and Reignault, P.** (2007) Correlative analysis of  
504 *Mycosphaerella graminicola* pathogenicity and cell wall-degrading enzymes produced in vitro: the  
505 importance of xylanase and polygalacturonase. *Plant Pathology*, **56**.
- 506 **Edgar, R.C.** (2004) MUSCLE. Multiple sequence alignment with high accuracy and high throughput.  
507 *Nucleic Acids Res*, **32**, 1792–1797.
- 508 **Fones, H. and Gurr, S.** (2015) The impact of Septoria tritici Blotch disease on wheat: An EU  
509 perspective. *Fungal genetics and biology : FG & B*, **79**, 3–7.
- 510 **Fox, E.M. Gardiner, D.M. Keller, N.P. and Howlett, B.J.** (2008) A Zn(II)2Cys6 DNA binding protein  
511 regulates the sirodesmin PL biosynthetic gene cluster in *Leptosphaeria maculans*. *Fungal Genet.*  
512 *Biol.* **45**, 671–682.

- 513 **Galhano, R. Illana, A. Ryder, L.S. Rodríguez-Romero, J. Demuez, M. Badaruddin, M. Martinez-**  
514 **Rocha, A.L. Soanes, D.M. Studholme, D.J. Talbot, N.J. and Sesma, A.** (2017) Tpc1 is an important  
515 Zn(II)2Cys6 transcriptional regulator required for polarized growth and virulence in the rice blast  
516 fungus. *PLoS Pathog*, **13**, e1006516.
- 517 **Gibson, D.G. Young, L. Chuang, R.-Y. Venter, J.C. Hutchison, C.A. and Smith, H.O.** (2009) Enzymatic  
518 assembly of DNA molecules up to several hundred kilobases. *Nature methods*, **6**, 343–345.
- 519 **Gohari, A.M. Ware, S.B. Wittenberg, Alexander H J, Mehrabi, R. M'Barek, S.B. Verstappen, Els C P,**  
520 **van der Lee, Theo A J, Robert, O. Schouten, H.J. de Wit, Pierre P J G M and Kema, G.H.** (2015)  
521 Effector discovery in the fungal wheat pathogen *Zymoseptoria tritici*. *Molecular Plant Pathology*,  
522 **16**, 931–945.
- 523 **Grandaubert, J. Dutheil, J.Y. and Stukenbrock, E.H.** (2017) The genomic determinants of adaptive  
524 evolution in a fungal pathogen.
- 525 **Habig, M. Kema, G. and Holtgrewe Stukenbrock, E.** (2018) Meiotic drive of female-inherited  
526 supernumerary chromosomes in a pathogenic fungus.
- 527 **Hartmann, F.E. Sanchez-Vallet, A. McDonald, B.A. and Croll, D.** (2017) A fungal wheat pathogen  
528 evolved host specialization by extensive chromosomal rearrangements. *The ISME journal*, **11**,  
529 1189–1204.
- 530 **Haueisen, J. Möller, M. Eschenbrenner, C.J. Grandaubert, J. Seybold, H. Adamiak, H. and**  
531 **Stukenbrock, E.H.** (2019) Highly flexible infection programs in a specialized wheat pathogen.  
532 *Ecology and evolution*, **9**, 275–294.
- 533 **Horton, P. Park, K.-J. Obayashi, T. Fujita, N. Harada, H. Adams-Collier, C.J. and Nakai, K.** (2007)  
534 WoLF PSORT. Protein localization predictor. *Nucleic Acids Res*, **35**, W585-7.
- 535 **Imazaki, I. Kurahashi, M. Iida, Y. and Tsuge, T.** (2007) Fow2, a Zn(II)2Cys6-type transcription  
536 regulator, controls plant infection of the vascular wilt fungus *Fusarium oxysporum*. *Molecular*  
537 *microbiology*, **63**, 737–753.
- 538 **Jing, H.-C. Lovell, D. Gutteridge, R. Jenk, D. Korniyukhin, D. Mitrofanova, O.P. Kema, Gert H. J. and**  
539 **Hammond-Kosack, K.E.** (2008) Phenotypic and genetic analysis of the *Triticum monococcum*-  
540 *Mycosphaerella graminicola* interaction. *New Phytol.* **179**, 1121–1132.
- 541 **Jones, J.D.G. and Dangl, J.L.** (2006) The plant immune system. *Nature*, **444**, 323–329.
- 542 **Kellner, R. Bhattacharyya, A. Poppe, S. Hsu, T.Y. Brem, R.B. and Stukenbrock, E.H.** (2014) Expression  
543 Profiling of the Wheat Pathogen *Zymoseptoria tritici* Reveals Genomic Patterns of Transcription  
544 and Host-Specific Regulatory Programs. *Genome Biol Evol*, **6**, 1353–1365.
- 545 **Kema, G.H. Verstappen, E.C. Todorova, M. and Waalwijk, C.** (1996) Successful crosses and molecular  
546 tetrad and progeny analyses demonstrate heterothallism in *Mycosphaerella graminicola*. *Curr*  
547 *Genet*, **30**, 251–258.
- 548 **Kema, G. H. J. Yu, D.Z. Rijkenberg, F. H. J. Shaw, M.W. and Baayen, R.P.** (1996) Histology of the  
549 pathogenesis of *Mycosphaerella graminicola* in wheat. *Phytopathology* **86**: 777-786.
- 550 **Lee, W.-S. Rudd, J.J. Hammond-Kosack, K.E. and Kanyuka, K.** (2014) *Mycosphaerella graminicola*  
551 LysM effector-mediated stealth pathogenesis subverts recognition through both CERK1 and CEBiP  
552 homologues in wheat. *Molecular plant-microbe interactions : MPMI*, **27**, 236–243.
- 553 **Lu, J. Cao, H. Zhang, L. Huang, P. and Lin, F.** (2014) Systematic analysis of Zn2Cys6 transcription  
554 factors required for development and pathogenicity by high-throughput gene knockout in the rice  
555 blast fungus. *PLoS Pathog*, **10**, e1004432.
- 556 **MacPherson, S. Larochele, M. and Turcotte, B.** (2006) A fungal family of transcriptional regulators:  
557 the zinc cluster proteins. *Microbiology and molecular biology reviews : MMBR*, **70**, 583–604.
- 558 **Marshall, R. Kombrink, A. Motteram, J. Loza-Reyes, E. Lucas, J. Hammond-Kosack, K.E. Thomma,**  
559 **Bart P H J and Rudd, J.J.** (2011) Analysis of two in planta expressed LysM effector homologs from



- 560 the fungus *Mycosphaerella graminicola* reveals novel functional properties and varying  
561 contributions to virulence on wheat. *Plant Physiol.* **156**, 756–769.
- 562 **Mirzadi Gohari, A. Mehrabi, R. Robert, O. Ince, I.A. Boeren, S. Schuster, M. Steinberg, G. de Wit,**  
563 **Pierre J. G. M. and Kema, Gert H. J.** (2014) Molecular characterization and functional analyses of  
564 ZtWor1, a transcriptional regulator of the fungal wheat pathogen *Zymoseptoria tritici*. *Molecular*  
565 *Plant Pathology*, **15**, 394–405.
- 566 **Mohammadi, N. Mehrabi, R. Gohari, A.M. Mohammadi Goltapeh, E. Safaie, N. and Kema, G.H.J.**  
567 (2017) The ZtVf1 transcription factor regulates development and virulence in the foliar wheat  
568 pathogen *Zymoseptoria tritici*. *Fungal Genetics and Biology*, **109**, 26–35.
- 569 **Möller, M. Habig, M. Freitag, M. and Stukenbrock, E.H.** (2018) Extraordinary Genome Instability and  
570 Widespread Chromosome Rearrangements During Vegetative Growth. *Genetics*.
- 571 **Morais, D. Géllisse, S. Laval, V. Sache, I. and Suffert, F.** (2016) Inferring the origin of primary  
572 inoculum of *Zymoseptoria tritici* from differential adaptation of resident and immigrant  
573 populations to wheat cultivars. *Eur J Plant Pathol*, **145**, 393–404.
- 574 **O’Driscoll, A. Doohan, F. and Mullins, E.** (2015) Exploring the utility of *Brachypodium distachyon* as a  
575 model pathosystem for the wheat pathogen *Zymoseptoria tritici*. *BMC Res Notes*, **8**, 132.
- 576 **Okmen, B. Collemare, J. Griffiths, S. van der Burgt, Ate, Cox, R. and Wit, P.J.G.M. de** (2014)  
577 Functional analysis of the conserved transcriptional regulator CfWor1 in *Cladosporium fulvum*  
578 reveals diverse roles in the virulence of plant pathogenic fungi. *Molecular microbiology*, **92**, 10–  
579 27.
- 580 **Orton, E.S. Deller, S. and Brown, James K M** (2011) *Mycosphaerella graminicola*: from genomics to  
581 disease control. *Mol. Plant Pathol.* **12**, 413–424.
- 582 **Pan, T. and Coleman, J.E.** (1990) GAL4 transcription factor is not a “zinc finger” but forms a Zn (II)  
583 2Cys6 binuclear cluster. *Proc. Natl. Acad. Sci. U.S.A.* **87**, 2077–2081.
- 584 **Park, J. Park, J. Jang, S. Kim, S. Kong, S. Choi, J. Ahn, K. Kim, J. Lee, S. Kim, S. Park, B. Jung, K. Kim, S.**  
585 **Kang, S. and Lee, Y.-H.** (2008) FTFD. An informatics pipeline supporting phylogenomic analysis of  
586 fungal transcription factors. *Bioinformatics (Oxford, England)*, **24**, 1024–1025.
- 587 **Ponomarenko A. S.B. Goodwin, G.H.J. Kema** (2011) *Septoria tritici* blotch (STB) of wheat.  
588 *10.1094/PHI*.
- 589 **Poppe, S. Dorsheimer, L. Happel, P. and Stukenbrock, E.H.** (2015) Rapidly Evolving Genes Are Key  
590 Players in Host Specialization and Virulence of the Fungal Wheat Pathogen *Zymoseptoria tritici*  
591 (*Mycosphaerella graminicola*). *PLoS pathogens*, **11**, e1005055.
- 592 **Quevillon, E. Silventoinen, V. Pillai, S. Harte, N. Mulder, N. Apweiler, R. and Lopez, R.** (2005)  
593 InterProScan. Protein domains identifier. *Nucleic Acids Res*, **33**, W116-20.
- 594 **R Core Team** (2015) R: A Language and Environment for Statistical Computing. Vienna, Austria.  
595 <https://www.R-project.org>.
- 596 **Rath, M. Grolig, F. Haueisen, J. and Imhof, S.** (2014) Combining microtomy and confocal laser  
597 scanning microscopy for structural analyses of plant-fungus associations. *Mycorrhiza*, **24**, 293–  
598 300.
- 599 **RStudio Team** (2015) RStudio: Integrated Development Environment for R. Boston, MA.  
600 <http://www.rstudio.com/>.
- 601 **Rudd, J.J. Kanyuka, K. Hassani-Pak, K. Derbyshire, M. Andongabo, A. Devonshire, J. Lysenko, A.**  
602 **Saqi, M. Desai, N.M. Powers, S.J. Hooper, J. Ambroso, L. Bharti, A. Farmer, A. Hammond-Kosack,**  
603 **K.E. Dietrich, R.A. and Courbot, M.** (2015) Transcriptome and metabolite profiling of the infection  
604 cycle of *Zymoseptoria tritici* on wheat reveals a biphasic interaction with plant immunity involving  
605 differential pathogen chromosomal contributions and a variation on the hemibiotrophic lifestyle  
606 definition. *PLANT PHYSIOLOGY*, **167**, 1158–1185.

- 607 **Rybak, K. See, P.T. Phan, H.T.T. Syme, R.A. Moffat, C.S. Oliver, R.P. and Tan, K.-C.** (2017) A  
608 functionally conserved Zn<sub>2</sub> Cys<sub>6</sub> binuclear cluster transcription factor class regulates necrotrophic  
609 effector gene expression and host-specific virulence of two major Pleosporales fungal pathogens  
610 of wheat. *Mol. Plant Pathol.* **18**, 420–434.
- 611 **Sambrook, J. and Russell, D.W.** (2001) *Molecular Cloning. A laboratory manual.* Gold Spring Harbor,  
612 New York: Gold Spring Harbor Laboratory Pr.
- 613 **Schneider, C.A. Rasband, W.S. and Eliceiri, K.W.** (2012) NIH Image to ImageJ. 25 years of image  
614 analysis. *Nat Meth*, **9**, 671–675.
- 615 **Siah, A. Deweer, C. Duyme, F. Sanssené, J. Durand, R. Halama, P. and Reignault, P.** (2010)  
616 Correlation of in planta endo-beta-1,4-xylanase activity with the necrotrophic phase of the  
617 hemibiotrophic fungus *Mycosphaerella graminicola*. *Plant Pathology*, **59**, 661–670.
- 618 **Somai-Jemali, L. Randoux, B. Siah, A. Magnin-Robert, M. Halama, P. Reignault, P. and Hamada,**  
619 **W.** (2017) Similar infection process and induced defense patterns during compatible interactions  
620 between *Zymoseptoria tritici* and both bread and durum wheat species. *Eur J Plant Pathol*, **147**,  
621 787–801.
- 622 **Son, H. Seo, Y.-S. Min, K. Park, A.R. Lee, J. Jin, J.-M. Lin, Y. Cao, P. Hong, S.-Y. Kim, E.-K. Lee, S.-H.**  
623 **Cho, A. Lee, S. Kim, M.-G. Kim, Y. Kim, J.-E. Kim, J.-C. Choi, G.J. Yun, S.-H. Lim, J.Y. Kim, M. Lee,**  
624 **Y.-H. Choi, Y.-D. and Lee, Y.-W.** (2011) A phenome-based functional analysis of transcription  
625 factors in the cereal head blight fungus, *Fusarium graminearum*. *PLoS Pathog.* **7**, e1002310.
- 626 **Southern, E.M.** (1975) Detection of specific sequences among DNA fragments separated by gel  
627 electrophoresis. *Journal of Molecular Biology*, **98**, 503–517.
- 628 **Stewart, E.L. Hagerty, C.H. Mikaberidze, A. Mundt, C.C. Zhong, Z. and McDonald, B.A.** (2016) An  
629 Improved Method for Measuring Quantitative Resistance to the Wheat Pathogen *Zymoseptoria*  
630 *tritici* Using High-Throughput Automated Image Analysis. *Phytopathology*, **106**, 782–788.
- 631 **Tukey, J.W.** (1949) Comparing Individual Means in the Analysis of Variance. *Biometrics*, **5**, 99.
- 632 **Xiong, D. Wang, Y. Tang, C. Fang, Y. Zou, J. and Tian, C.** (2015) VdCrz1 is involved in microsclerotia  
633 formation and required for full virulence in *Verticillium dahliae*. *Fungal Genet. Biol.* **82**, 201–212.
- 634 **Yemelin, A. Brauchler, A. Jacob, S. Laufer, J. Heck, L. Foster, A.J. Antelo, L. Andresen, K. and Thines,**  
635 **E.** (2017) Identification of factors involved in dimorphism and pathogenicity of *Zymoseptoria*  
636 *tritici*. *PLoS ONE*, **12**, e0183065.
- 637 **Zhang, W.-Q. Gui, Y.-J. Short, D.P.G. Li, T.-G. Zhang, D.-D. Zhou, L. Liu, C. Bao, Y.-M. Subbarao, K.V.**  
638 **Chen, J.-Y. and Dai, X.-F.** (2018) *Verticillium dahliae* transcription factor VdFTF1 regulates the  
639 expression of multiple secreted virulence factors and is required for full virulence in cotton. *Mol.*  
640 *Plant Pathol.* **19**, 841–857.
- 641 **Zhong, Z. Marcel, T.C. Hartmann, F.E. Ma, X. Plissonneau, C. Zala, M. Ducasse, A. Confais, J.**  
642 **Compain, J. Lapalu, N. Amselem, J. McDonald, B.A. Croll, D. and Palma-Guerrero, J.** (2017) A  
643 small secreted protein in *Zymoseptoria tritici* is responsible for avirulence on wheat cultivars  
644 carrying the *Stb6* resistance gene. *The New phytologist*, **214(2)**, 619–631.
- 645 **Zhuang, Z. Lohmar, J.M. Satterlee, T. Cary, J.W. and Calvo, A.M.** (2016) The Master Transcription  
646 Factor *mtfA* Governs Aflatoxin Production, Morphological Development and Pathogenicity in the  
647 Fungus *Aspergillus flavus*. *Toxins*, **8**.
- 648 **Zwiers, L.-H. and De Waard, Maarten A.** (2001) Efficient *Agrobacterium tumefaciens*-mediated gene  
649 disruption in the phytopathogen *Mycosphaerella graminicola*. *Current Genetics*, **39**, 388–393.
- 650
- 651

## 652 **Supporting Information legends**

653

654 **Figure S1. In vitro phenotype of *Zt107320* mutants.** *In vitro* growth of the wildtype (wt), two  
655 independent deletion strains ( $\Delta Zt107320$ ), two independent complementation strains  
656 ( $\Delta Zt107320::Zt107320\_eGFP$ ) on YMS media including the indicated compounds to assess the effect  
657 of osmotic stress (NaCl, Sorbitol) , reactive oxygen species ( $H_2O_2$ ), cell wall stressors (Calcofluor,  
658 Congo Red) and increased temperature (28°C) on growth and morphology of *Z. tritici*.

659

660 **Figure S2. Growth morphologies of *Z. tritici* wildtype and  $\Delta Zt107320$  and  $\Delta Zt107320::Zt107320-$**   
661 ***eGFP* strains on minimum medium in the presence of different carbon sources.** Growth depicted  
662 after a) 7 days and b) 14 days. After 7 days, and more pronounced after 14 days of incubation, a  
663 higher amount of hyphal growth is observed for the  $\Delta Zt107320$  mutants on the carbon sources  
664 Fructose, Galactose, Glucose, Maltose, Sorbitol, Sucrose and Xylose.

665

666 **Figure S3. Generation of *Zt107320* mutants in *Z. tritici*.** a) Schematic illustration of the gene  
667 replacement strategy of *Zt107320*. Generation of the  $\Delta Zt107320$  strains by homologous  
668 recombination between the upstream (UF) and downstream flanking regions (DF) of *Zt107320* in its  
669 genomic locus and a plasmid carrying the hygromycin resistance cassette (*hygR*) located between the  
670 UF and DF. Homologous recombination results in the integration of the hygromycin-resistance gene  
671 cassette (*hygR*) in the locus of *Zt107320*.  $\Delta Zt107320::Zt107300-eGFP$  were generated by homologous  
672 recombination between UF and DF of the  $\Delta Zt107320$  strains and a transformed plasmid containing a  
673 c-terminal fusion of *Zt107320* and *eGFP* and a Geneticin resistance cassette (*NeoR*) located between  
674 the UF and DF Yellow bars indicate the position of the probes used in the Southern blot analyses. b)  
675 Confirmation of *Zt107320* mutants by Southern blot analyses.

676

677 **Table S1: List of all primers used within this study**

678 **Table S2: Summary of *in vitro* growth data**

679 **Table S3: Summary of *in planta* phenotype**